JOURNAL OF SPACECRAFT AND ROCKETS
Vol. 32, No. 2, March–April 1995

Design, Analysis, and Testing of an Aerobrake Test Model

K. N. Shivakumar,* V. S. Avva,† R. L. Sadler,‡ A. Farouk,§ and J. C. Riddick¶
North Carolina A&T State University, Greensboro, North Carolina 27411

A one-tenth-scale test model of a spherical sandwich aerobrake proposed for a lunar transfer vehicle was developed. The objective of this paper is to demonstrate the structural integrity of this aerobrake test model. Membrane stress analysis and the idea of equal stress/strength ratio of the skin material were used in the design. The test model had an outer radius of 4.45 ft (1.36 m), a base diameter of 5 ft (1.5 m), and a total wall thickness of 0.9 in (23 mm). The sandwich shell wall was made out of glass/polyester resin skin and polyvinyl foam core. An air-pressure test was conducted. The measured displacements and strains agreed well with the finite element analysis results. The aerobrake model survived 160% of the design pressure with no structural failure.

Nomenclature

c = base radius of the aerobrake test model, in.
d = total thickness of the shell wall, in.
E = elastic modulus, psi
p = pressure at any point on the surface of the shell, psi
p_0 = stagnation pressure, psi
R = mean radius, in.
S = material strength, psi
t = thickness of the shell, in.
ν = Poisson's ratio of the material
σ = stress, psi
ϕ = spherical angle, deg
ϕ_1 = spherical angle between the apex and support ring of the shell, deg
ϕ_2 = spherical angle between the apex and outer edge of the shell, deg

Subscripts

core = core material
m = model
s = structure
skin = skin material
θ = hoop direction
ϕ = meridional direction

Introduction

ESTABLISHMENT of a lunar colony is considered a precursor to a human mission to Mars and other planets. The transportation of materials and personnel from Earth to the moon is a major technical challenge because of the exorbitant cost of delivering payloads to Earth orbit. One method of reducing the total transportation cost is by a space-based reusable interplanetary transfer vehicle. In a lunar mission, the space-based lunar transfer vehicle (LTV) could reside at the Space Station Freedom and transfer payloads between the Space Station and the moon.

The LTV or similar transfer vehicles experience large changes in velocity between interplanetary transfer orbit and Earth parking orbit. These maneuvers are called capture. Propulsive braking and aerobraking are the two techniques currently suggested for capture of transfer vehicles. In a propulsive capture, propellant required for a round trip to the moon and return must be carried, which adds to the weight of the vehicle. In an aerobraking capture, the velocity of the vehicle is reduced by the aerodynamic drag created when the spacecraft enters the Earth's atmosphere. Therefore, aerobraking reduces the fuel required for the mission. Because the aerobrake can be made reusable, it could reduce the ground launch cost for multiple-orbital-transfer missions. Generally, an aerobrake is considered advantageous only if the aerobrake mass is less than the avoided propellant and propulsion-system mass. Aerobraking is found to be economic if the mass of the aerobrake is less than 15% of the mass of the transfer vehicle.[1–3]

Analysis and design of aerobrakes constitute a multidisciplinary program involving aerodynamics, heat transfer, and structural analyses. Aerodynamic and heat-transfer analyses are required for calculating aerodynamic drag, pressure, and thermal loads, and structural analysis is required to design the aerobrake to withstand aerothermal loads. A number of studies have been reported on aerobrake types, shapes, and constructions for various missions.[1–11] This study is meant to demonstrate the design, fabrication, test, and analysis verification of a one-tenth-scale aerobrake proposed for lunar-transfer return vehicles.[1–3] A detailed stress analysis and optimization of this aerobrake were reported in Refs. 10 and 11. Figure 1 shows a proposed LTV aerobrake configuration and the aerodynamic loading during an entry into Earth orbit. The aerobrake is assumed to be constructed of sandwich graphite-epoxy composite. A one-tenth-scale test model of the aerobrake was developed using kinematically compatible dimensional analysis. The model was fabricated using glass/polyester resin laminate as skin, and polyvinyl chloride foam as core. Pressure tests were conducted, and the measured displacements and strains are compared with a finite element solution.

LTV Aerobrake Configuration and Loading

Figure 1 shows a proposed aerobrake for lunar-transfer return vehicles.[1–3] The aerobrake is a spherical shell with a radius of 44.5 ft and a base diameter of 50 ft. The aerobrake wall is made of 8-ply (0.04-in., 1-mm) graphite-epoxy skin and 2-in. (51-mm) graphite-epoxy honeycomb core. A Newtonian mechanics calculation for a spherical shell of mass 45,000 lb (weight 210 kN) entering the Earth's atmosphere at an altitude of 200,000 ft (60,960 m) with a deceleration of $5g$ resulted in a stagnation pressure p_0 of 1.04 psi (7.2 kPa). The pressure distribution on out side surface of the shell follows a cosine-squared formula, $p_0 = p\cos^2\phi$. The equivalent uniform pressure on the aerobrake is about 0.84 psi (5.8 kPa). Previous studies[10,11] have shown that the equivalent uniform pressure would reduce the maximum stress by 9% and increase the buckling load by 3%. However, the locations of the maximum stress and the buckling mode were the same for both cases. Because we can assume the above differences are small and because of the ease of

Received March 3, 1994; revision received July 22, 1994; accepted for publication Oct. 7, 1994.

*Research Professor, Department of Mechanical Engineering. Associate Fellow AIAA.
†Professor, Department of Mechanical Engineering.
‡Adjunct Associate Professor, Department of Mechanical Engineering.
§Former Adjunct Assistant Professor, Department of Mechanical Engineering.
¶Graduate Student, Department of Mechanical Engineering; currently Graduate Student, Virginia Polytechnic Institute and State University, Blacksburg, VA.

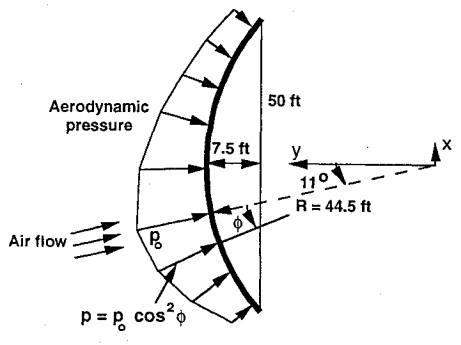

Fig. 1 Proposed LTV aerobrake configuration and loading.

applying uniform pressure, the test model was designed and tested for uniform pressure. The vehicle payload is assumed to be attached to the aerobrake through a ring beam.

Design of Test Model

The test model was designed so that the ratio of the maximum stress to the material strength of the model and the aerobrake structure is the same. Note that the word structure and the subscript s refer to the full-scale aerobrake structure, and the word model and the subscript m refer to the test model. Membrane stress analysis was used to calculate hoop (σ_θ) and meridional (σ_ϕ) stresses. Figure 2 shows the idealized configuration of the aerobrake with ring support and a uniform pressure load p. The membrane stress expressions[12] are given in two parts:

1) Between the apex and the support,

$$\sigma_\theta = \sigma_\phi = \frac{pR}{2t} \qquad \text{for} \quad 0 \le \phi \le \phi_1 \tag{1}$$

2) Between the support and the outer edge,

$$\sigma_\theta = -\frac{pR}{2t}\left(\frac{\sin^2\phi + \sin^2\phi_2}{\sin^2\phi_1}\right)$$
$$\sigma_\phi = -\frac{pR}{2t}\left(\frac{\sin^2\phi - \sin^2\phi_2}{\sin^2\phi_1}\right) \tag{2}$$

for $\phi_1 \le \phi \le \phi_2$.

Here ϕ is the spherical angle measured between the apex and any point on the shell. Note that at the support ($\phi = \phi_1$), Eqs. (1) and (2) show discontinuous stress due to the contributions from the support reactions. Although the membrane equations are not accurate at and near the support, they can be used to apply the kinematic similarity conditions between the structure and the test model. Figure 3 shows the distribution of σ_ϕ and σ_θ along the spherical angle ϕ for an arbitrary value of $\phi_1 = 10$ deg. The two stresses are constant and identical between the shell apex and the support (see the left side of the vertical support line in Fig. 3). Immediately beyond the support, both σ_ϕ and σ_θ peaked (with opposite signs), and then decreased monotonically towards the outer edge of the shell. It can be shown from Eqs. (1) and (2) that the broken curved lines represent the support stresses if the support is moved towards the apex of the shell. On the other hand, the support stresses decrease if the support is moved towards the outer edge of the shell. The support stresses are small and almost reach a plateau for $\phi_1 > 25$ deg. Therefore, the support location was chosen to be at $\phi_1 = 25.5$ deg, which corresponds to 75% span location (see broken vertical line). More details of the stress analysis can be found in Refs. 8, 10, and 11.

Of the two stresses, the hoop stress is the larger (see Fig. 3), and its value at the support was used in the design. For the test model and the structure to have an equal ratio of maximum stress to material strength, we can write

$$\left(\frac{pR}{2tS}\right)_m = \left(\frac{pR}{2tS}\right)_s \tag{3}$$

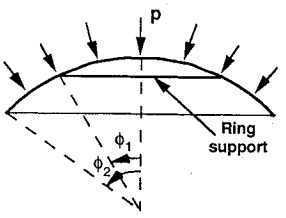

Fig. 2 Idealized spherical shell subjected to a pressure p with a ring support at ϕ_1.

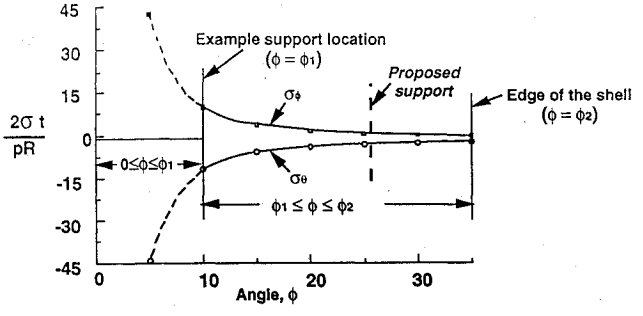

Fig. 3 Membrane stress distribution along the meridian of a spherical shell.

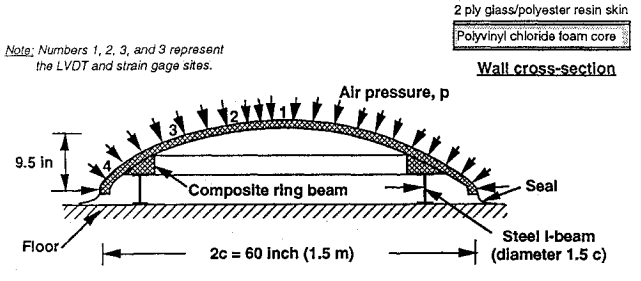

Fig. 4 Aerobrake test model with support beam and edge sealing.

The aerobrake structure properties are $S_s = 88$ ksi (606 MPa), $t_s = 0.08$ in. (2 mm), and $R_s = 44.5$ ft (13.6 m). The radius R_m and the material strength S_m of the test model are 4.45 ft (1.36 m) and 14 ksi (96.5 MPa), respectively. Simplification of Eq. (3) leads to a relation between the pressure and the thickness of the test model,

$$p_m = 16.7 t_m \tag{4}$$

For a test pressure of 1 psi (6.89 kPa), the model thickness is 0.06 in. (1.5 mm). Because sandwich construction was chosen, two layers of glass mat were used to make the skins have uniform properties. The final fabricated thickness of each of the skins was 0.075 in. (1.9 mm), and the total thickness was 0.15 in. (3.8 mm). According to Eq. (4), the test design pressure is 2.5 psi (17 kPa).

The core thickness of the model was selected to allow no buckling during the test. A $\frac{5}{8}$-in. (16-mm) polyvinyl chloride foam was chosen (from the available stock) as a core material. The total thickness d of the test model was 0.78 in. (20 mm). The buckling pressure for externally pressurized spherical shells is given[13] by

$$p_{\text{buckling}} = \frac{2tdE}{R^2 \dfrac{\sin^2\phi_1 + \sin^2\phi_2}{\sin^2\phi_1}} \tag{5}$$

Substituting the configuration properties of the test model and assuming $E_{\text{skin}} = 0.92$ Msi (6.34 GPa), the calculated buckling pressure is 28.4 psi (196 kPa). Figure 4 shows the test model configuration, support location, and loading. The base diameter ($2c$) of the shell is 60 in. (1.5 m), its height is 9.5 in. (241 mm), and its radius is 53.4 in. (1.36 m). The insert sketch shows the wall construction of the model. The figure also shows the four locations where the LVDTs (linearly variable displacement transformers) and strain gauges are mounted.

Fabrication of Aerobrake Model

The fabrication of the aerobrake model consists of construction of the mold pattern, the mold, and then the test model. A brief description of each step in the fabrication process is presented in the following subsections.

Mold Pattern

After the sandwich aerobrake model configuration was established, a wooden pattern was constructed. A hole was drilled in the apex of the pattern so that air pressure could be used between the pattern and the mold to aid in mold-pattern separation, if required. The wooden pattern was sealed with polyurethane varnish, sanded, and sealed again. The pattern was then coated with several coats of Trewax, with a buffing after each application. After the final coat of wax was buffed, a solution of polyvinyl alcohol mold release was sprayed on the pattern to form an even green plastic film.

Mold Construction

Randomly chopped fiberglass mat ($1\frac{1}{2}$ oz/ft^2) was cut into six pie sections, to fit the contour of the pattern. Polyester laminating resin was catalyzed with 1% methyl ethyl ketone peroxide catalyst, which provided approximately 30 min of pot life for application. The catalyzed polyester resin was brushed on a section of the pattern, the pie section of mat was pressed into the resin, and additional resin was brushed over the top of the fiberglass mat. The impregnated mat was then rolled with a ribbed roller tool to eliminate trapped air between the impregnated mat and the pattern. As soon as one section was completed, the same procedure was applied to the adjacent section. This was continued around the pattern until the entire pattern was covered. The polyester resin was then allowed to cure overnight, and the second layer (ply) was added in the same manner. To reduce the tendency of the mold to distort into an ellipse, a stiffener was added to the flange before the third and final ply was applied. For this stiffener, a $\frac{1}{2}$-in. layer of polyurethane foam was cut to fit the flange and bonded to the fiberglass composite with the same polyester resin. Finally, the top ply of fiberglass was applied to cover the entire surface of the mold. After curing for several days, the mold was removed from the pattern and the edges were trimmed. The inner surface of the mold was then wet-sanded to remove minor surface defects and finally polished for a good finish.

Aerobrake Model Construction

The model was built in three stages. First the outer skin was laminated, then the inner core was bonded, and finally the inner skin was applied to the bonded core. The support beam was bonded last. Fiberglass mat ($\frac{3}{4}$ oz/ft^2) was used for fabrication of aerobrake skin and the support beam.

Outer Skin

As in the case of the pattern, two coats of Trewax were applied to the mold and buffed to a polish finish. A coat of polyvinyl alcohol mold release agent was sprayed onto the waxed mold surface. Fiberglass mat was cut into pie sections and placed in the mold. The catalyzed polyester resin was applied, and the first ply of the aerobrake model was constructed. The resin application was minimized to reduce the weight and thickness of each ply. The second ply was added before the first ply was cured. The second-ply pie-section joints were staggered to minimize their effect. After the outside plies were cured, the exposed surface of the composite was rough sanded to remove any burrs or stray fibers that extended above the primary surface.

Inner Core and Inner Skin

Aircraft-grade, 3-lb/ft^3, $\frac{5}{8}$-in.-thick polyvinyl chloride foam was used as the core. The core material as supplied was cut into $1\frac{1}{8}$-in. squares with a bonded woven backing to provide the necessary draping formability to fit the mold contour. The core was cut into pie sections to fit exactly the inside surface contour of the aerobrake outside skin. Figure 5 illustrates the core pie sections being fitted into the inside of the aerobrake outside skin. The thixotropic polyester adhesive was applied to the inside of the aerobrake outside skin, and the core pressed into place. The mold-skin-adhesive-core assembly was placed in a nylon film vacuum bag, and a vacuum was applied until the adhesive was set. The bag was removed, and the excess adhesive was removed. The procedure for fabricating the inside skin was essentially the same as that for the outside skin. The finished thickness of the inner and outer skin was 0.075 in. (1.9 mm), and of the core was 0.75 in. (19 mm).

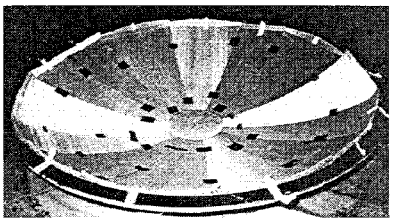

Fig. 5 Polyvinyl core sections laid over the outer skin of the aerobrake model.

Fig. 6 Completed aerobrake model with a rolled steel I-beam fitted.

Support Beam

Two plies of fiberglass mat about 4 in. wide were applied as a base for the support structure. A section of the polyvinyl foam core $1\frac{1}{2}$ in. thick was machined to fit the inside contour of the aerobrake skin. The machined foam core was bonded into the inside of the aerobrake shell on top of the two plies of support structure. The foam sections were then covered with two plies of fiberglass mat by the same laminating procedure as used to fabricate the aerobrake skins.

Fitting the Steel Support Ring Beam

The aerobrake structure was mated with a rolled steel support beam. To improve the fit between the aerobrake and the support structure, the aerobrake and the steel ring were laid together, aligned, and leveled. Then the liquid resin and fiberglass mat were used to fill the gap. The steel beam was mold released so that it could be separated from the aerobrake after the resin is cured. This procedure provided very good contact between the aerobrake and the steel support beam. Figure 6 illustrates the steel support beam on the aerobrake model.

Material Properties

The material properties supplied by the manufacturer for glass–polyester-resin (mat) laminate and polyvinyl core are listed here.

1) *Skin properties* (isotropic): $E_{skin} = 0.92$ Msi (6.34 GPa), $\nu_{skin} = 0.14$, and tensile strength $S_{skin} = 14$ ksi (96.5 MPa).

2) *Core properties* (isotropic): $E_{core} = 3.4$ ksi (23.4 MPa) and $\nu_{core} = 0.14$.

Because of variability in the manufacturing process, particularly in a hand layup procedure, the laminate elastic properties would be different from those suggested by the manufacturer. Therefore, a 10% variation of the elastic modulus (E_{skin}) of the laminate was assumed, and its effects on computed displacements and strains were evaluated.

Aerobrake Test

Test Setup

Figure 7 shows the test setup and instrumentation of the aerobrake model. The model is supported on a circular rolled steel I beam (see Fig. 4), which is resting on a clean, flat, and smooth floor.

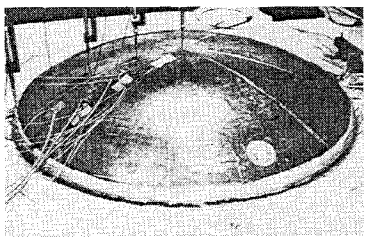

Fig. 7 Aerobrake model test setup.

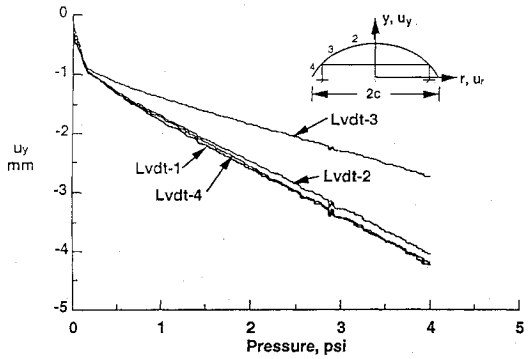

Fig. 8 Variation of measured displacement u_y with applied pressure at four locations along the meridian of the aerobrake.

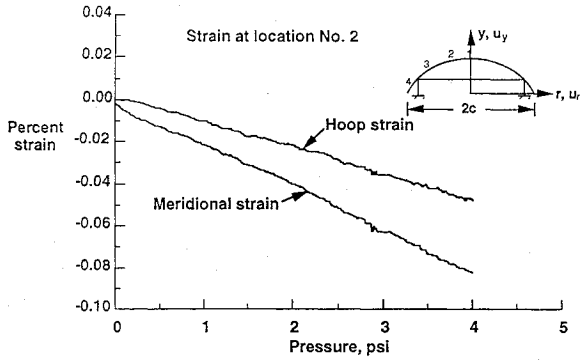

Fig. 9 Variation of hoop and meridional strain with pressure at location 2 on the meridian.

The gap (about 1 in.) between the aerobrake edge and the floor was sealed by an annular plastic sheet using a vacuum-bag sealing compound. Before sealing, a piezoelectric pressure transducer was placed inside the model and its terminals were connected to the data acquisition system. Two hoses, one for the air inlet and the other for air outlet, were also placed between the aerobrake and the floor for air evacuation and ventilation. The air outlet hose was connected to a vacuum pump. Because the model is axisymmetric, instruments are mounted on a meridian of the shell. Four LVDTs were mounted at four locations on the meridian of the model. These locations were at about 0.0, 8 (203), 15 (381), and 28.6 (726) in. (mm) from the apex of the model. Near each of these locations, two strain gauges were mounted—one along the meridian and the other along the hoop direction. All LVDTs and strain gauges were connected to an automatic data acquisition system. All instruments were initialized and calibrated.

Test Procedure

External pressure was applied by evacuating the air between the inside surface of the aerobrake and the floor. The vacuum pump was switched on, and the air outlet and inlet valves were adjusted so that a smooth and continuous increase in the air pressure was applied on the aerobrake. The air pressure, vertical displacements (u_y), and strains were recorded at 2-s intervals. The air evacuation was continued to a pressure of about 2 psi (14 kPa). Then the pressure was released by switching off the pump and opening the air inlet valve. The unloading profile of the displacement-pressure curve did not exactly match the loading curve, because of the hysteresis in the test system. The loading and unloading process were repeated five times before the final test. After allowing the test setup to relax for about one-half hour, the final two tests were conducted up to a pressure of about 4 psi (28 kPa). The two consecutive tests were conducted to verify the repeatability of the test results. The pressurization to 4 psi took about 5 min.

Test Results

Figure 8 shows the measured variation of the vertical displacement u_y with the applied pressure. The initial nonlinear behavior of the curve is due to support deformation and other initial deformations that are expected in this type of test setup. The roughness in the curves was due to the data-acquisition-system noise and the high frequency (2-s intervals) of data recording. All four curves are almost straight except at pressures less than 0.3 psi (2 kPa), which is an indication that there is no structural failure in the model even at 4-psi (28-kPa) pressure. That pressure is about 160% of the design pressure (2.5 psi, 17 kPa) of the aerobrake test model. The initial nonlinear portion of the displacement u_y was eliminated in calculating the final displacements. The average (of two tests) displacements at 4-psi (28-kPa) pressure were −3.6, −3.4, −2.1, and −3.5 mm, respectively at the four locations (see nos. 1 to 4 in the Fig. 8 insert). Figure 9 shows the variation of hoop and meridional strains at location 2 with the pressure. Note that both curves are almost linear, which further confirms that no damage occurred up to 4-psi (28-kPa) pressure. The response of the other six strain gages at the other three locations was generally similar; therefore, it is not presented here.

Analysis

Finite Element Model

The stress analysis of the aerobrake test model subjected to a uniform pressure was conducted using a commercial finite element code ANSYS.[14] Because the configuration, support conditions, and the loading are axisymmetric, an axisymmetric analysis was performed. Figure 10 shows the finite element idealization of the aerobrake using eight-node, isoparametric, parabolic axisymmetric elements. Note that the thickness dimension is scaled up five times for clarity of the picture. The meridional length is divided into 45 equal parts and the thickness is divided into five parts, with two divisions in each of the two skins. The support-beam idealization is also shown in Fig. 10. The aerobrake skirt (about 1-in., or 25-mm, projection) and the gap between the aerobrake and the floor (about 1 in., or 25 mm) were also modeled as a skin material. The idealization had 369 eight-node isoparametric elements. Compressive pressure load on the model was applied as a consistent load vector at the nodes. A mesh refinement study was conducted by simply doubling the number of divisions used above. Calculated displacements and strains were almost identical (less than 1% difference) to those obtained from the original mesh. Hence, the 369-element idealization was used for all analysis. As mentioned previously (owing to uncertainty of the material properties) the modulus of elasticity of the aerobrake skin material (E_{skin}) was assumed to vary by 10% from the manufacturer's suggested value (0.92 Msi, or 6.34 GPa). Therefore, the stress analysis was conducted for E_{skin} values of 0.83 (5.7), 0.92 (6.34), and 1.01 (7.0) Msi (GPa).

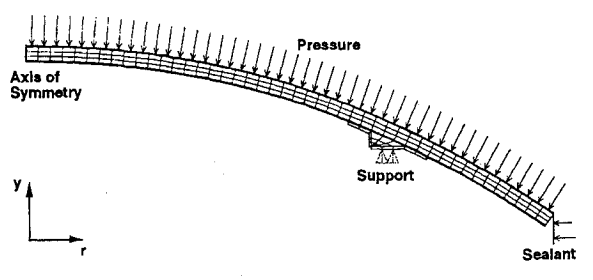

Fig. 10 Finite element model, loading, and support conditions.

Analytical and Experimental Comparison

Figure 11 shows the deformed configuration of the aerobrake model at 1-psi (6.89-kPa) pressure. All displacements were scaled by 35 times to give a better description of the deformation. Figure 12 shows the variation of the displacement u_y along the meridian of the model. The radial axis is normalized by the base radius of the aerobrake. The apex and the outer edge of aerobrake are represented by $r/c = 0.0$ and $r/c = 1$, respectively. The figure shows the results for all three values of the modulus (a ±10% variation from the handbook value) of the skin material. Since the stiffness of the core is very small, all three curves appear to be scaled up or down according to E_{skin}. The two test results are shown by circle and triangle symbols. The excellent agreement between the two tests shows the repeatability of the test data. At all four locations the test results agree well with the analysis for $E_{skin} = 0.83$ Msi (5.7 GPa).

Figures 13 and 14 show the variation of hoop and meridional strains along r/c axis of the model. Again, results for three values of E_{skin} are presented. A wiggle in the meridional strain near the support was due to the additional layers of glass-polyester mat applied around the support beam. The horizontal broken line represents the strain at the apex ($r/c = 0$) calculated from the membrane analysis. The test data are represented by symbols. The test data agreed reasonably well with the analysis, except at the apex. Because the strains are functions of the local radius of curvature, thickness, and elastic modulus, they are more sensitive to the local variations of these parameters than the displacements are. In a hand layup fabrication process, local variation of thickness, curvature, and material properties are expected. Therefore, it is suggested to measure the elastic properties of the material from coupons cut from representative areas of the structure, and then use the measured material properties in the analysis to get a better correlation between the analysis and the test.

The hoop strain gauge near the edge of the shell (see Fig. 13) and the meridional strain gauge at location 3 (see Fig. 14) had some problems. The analysis and the test data at these locations could not be reconciled.

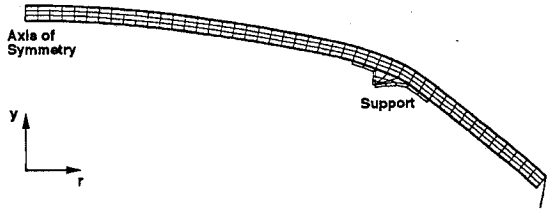

Fig. 11 Deformed shape of the aerobrake.

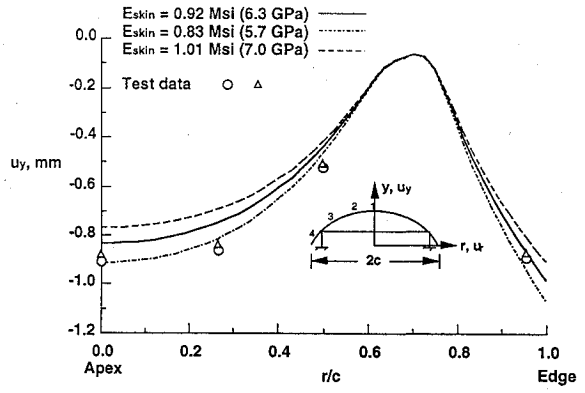

Fig. 12 Variation of displacement u_y along the meridian of the aerobrake.

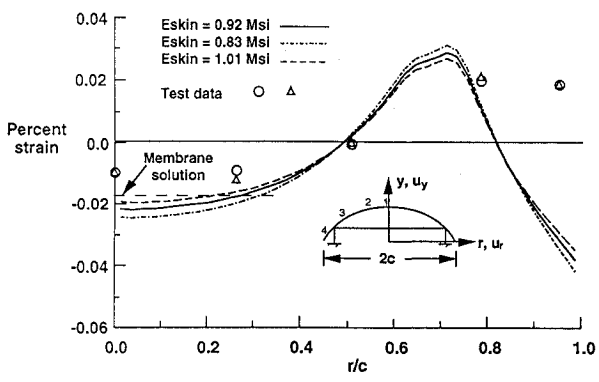

Fig. 13 Variation of hoop strain along the meridian of the aerobrake.

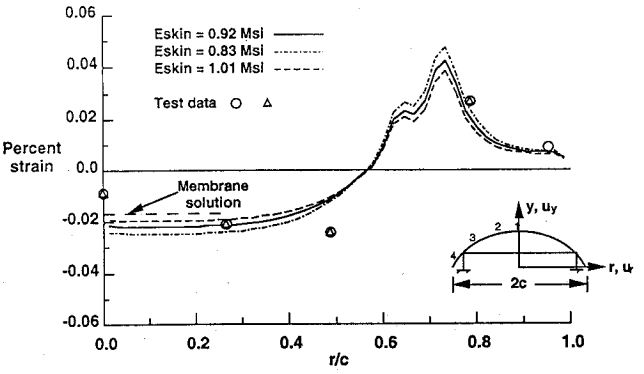

Fig. 14 Variation of meridional strain along the meridian of the aerobrake.

Concluding Remarks

A one-tenth-scale test model of a spherical sandwich aerobrake proposed for a lunar transfer vehicle was developed. The objective of this paper was to demonstrate the structural integrity of this aerobrake test model. Membrane stress analysis and the idea of equal stress/strength ratio of the skin material were used in the design. The test model had an outer radius of 4.45 ft (1.36 m), a base diameter of 5 ft (1.5 m), and a total wall thickness of 0.9 in. (23 mm). The sandwich shell wall was made out of glass/polyester resin skin and polyvinyl foam core. An air-pressure test was conducted. The measured displacements and strains agreed well with the finite element analysis results. The aerobrake model survived 160% of the design pressure with no structural failure. Because the strains are functions of local values of radius, thickness, and material stacking, local variation of material properties has to be included in the analysis to get a better correlation between the analysis and test.

Acknowledgments

The authors acknowledge the financial support of the Mars Mission Research Center, established by Grant NAGW-1331 from NASA, Washington, DC, and the computational support of the North Carolina Supercomputing Center, Research Triangle Park, NC.

References

[1]Rehder, J. J., Cruz, C. I., Braun, K. E., and Bush, L. B., "An Aerobrake Concept for Lunar Return," NASA TP-3262, Dec. 1992.

[2]Ball, J. M., Komerska, R. J., and Rawell, L. F., "Importance of Operations, Risk, and Cost Assessment of Space Transfer Vehicle Systems Design," AIF-92-0847, 1992.

[3]Katzberg, S. J., Butler, D. H., Doggett, W. R., Russell, J. W., and Hurban, T., "Aerobrake Assembly with Minimum Space Station Accommodation," NASA TM-102778, Oct. 1990.

[4]Dorsey, J. T., and Mikulas, M. M., Jr., "Preliminary Design of a Large Tetrahedral Truss/Hexagonal Heatshield Panel Aerobrake," NASA TM 101612, Sept. 1989.

[5]Washington, G., and Klang, E., "Modeling and Analysis of Doubly Curved Aerobrake Truss Structures," *Proceedings of the 3rd International Conference on Engineering, Construction, and Operations in Space*, SPACE '92, Denver, CO, May 1992.

[6]Raju, I. S., and Craft, W. J., "Analysis and Sizing of a Mars Aerobrake Structure," *Journal of Spacecraft and Rockets*, Vol. 30, No. 1, 1993, pp. 102–110.

[7]Dorsey, J., Watson, J., and Tutterow, R., "Structural Concepts for Lunar Transfer Vehicle Aerobrake Which Can Be Assembled on Orbit," AIAA Paper 93-1394, 1993.

[8]Hairr, J., and Klang, E., "Structural Considerations in the Design of a Mars Mission Aerobrake," *Proceedings of the 3rd International Conference on Engineering, Construction, and Operations in Space*, SPACE '92, Denver, CO, May 1992.

[9]Bush, L. B., and Unal, R., "Preliminary Structural Design of a Lunar Transfer Vehicle Aerobrake," AIAA Paper 92-1108, 1992.

[10]Shivakumar, K. N., Craft, W. J., and Riddick, J. C., "Mass Estimation of Lunar Aerobrake Models Made Up of Various Aerospace Materials," *Space Exploration Science and Technologies Research*, edited by W. J. Craft and D. M. Achgill, AD-Vol. 31, American Society of Mechanical Engineers, 1992, pp. 83–94.

[11]Shivakumar, K. N., and Riddick, J. C., "Minimum Mass Design of Sandwich Aerobrakes for a Lunar Transfer Vehicle," *Journal of Spacecraft and Rockets* (to be published).

[12]Timoshenko, S., and Woinowsky-Krieger, S., *Theory of Plates and Shells*, 2nd ed., McGraw-Hill, New York, 1959.

[13]Volmir, A. S., "A Translation of Flexible Plates and Shells," Air Force Flight Dynamics Laboratory, AFFDL-TR-66-216, April 1967.

[14]DeSalvo, G. J., and Gorman, R. W., *ANSYS Engineering Analysis System User's Manual*, Version 4.4, Swanson Analysis Systems, Inc., Houston, PA, May 1989.

I. E. Vas
Associate Editor